

**A**  
**THESIS REPORT**  
**ON**  
**“Thermal Modelling of Wire Arc Additive Manufacturing using Finite Element Method  
and Machine Learning”**

*Submitted in partial fulfilment of the  
Requirements for the award of the degree  
of*

**BACHELOR OF TECHNOLOGY**

*in*

**PRODUCTION ENGINEERING**

*by*

**UJJWAL KUMAR  
(19030520066)**

**DHARMENDAR KUMAR MAHATO  
(19030525003)**



**DEPARTMENT OF PRODUCTION ENGINEERING**

**B.I.T. SINDRI**

**SINDRI – 828123 (INDIA)**

**MAY, 2023**

## CANDIDATE'S DECLARATION

---

I hereby declare that the work carried out in this report titled “**Thermal Modelling Analysis of Wire Arc Additive Manufacturing using Finite Element Method and Machine Learning**” is presented on behalf of partial fulfilment of the requirements for the award of the degree of **Bachelor of Technology** with specialization in **Production Engineering** submitted to the department of **Production Engineering, B.I.T. Sindri, India**, under the supervision and guidance of **Prof. Mukesh Chandra**, Assistant Professor, Production Engineering, B.I.T. Sindri, India.

I have not submitted the matter embodied in this report for the award of any other degree or diploma.

Date: 6<sup>th</sup> May, 2023

**Ujjwal Kumar - 19030520066**

Place: **BIT Sindri**

**Dharmendar Kumar Mahato - 19030525003**



## **B.I.T. SINDRI**

(DEPARTMENT OF SCIENCE & TECHNOLOGY, GOVT. OF JHARKHAND, RANCHI)

P.O. SINDRI INSTITUTE, DHANBAD-828123

### **DECLARATION CERTIFICATE**

This is to certify that the work presented in this thesis entitled “**Thermal Modelling of Wire Arc Additive Manufacturing Using Finite Element Method and Machine Learning**” submitted by **Ujjwal Kumar and Dharmendar Kumar Mahato**, under supervision and guidance of **Prof. Mukesh Chandra**, Assistant Professor, Production Engineering, B.I.T. Sindri, India.

To the best of my knowledge, the content of this dissertation does not form a basis of the award of any previous degree to anyone else.

Prof. Mukesh Chandra,  
Assistant Professor,  
Production Engineering

Dr. Prakash Kumar,  
Head of Department,  
Production Engineering



**B.I.T. SINDRI**

### **CERTIFICATE OF APPROVAL**

The forgoing thesis entitled “**Thermal Modelling of Wire Arc Additive Manufacturing using Finite Element Method and Machine Learning**” is here by approved as a creditable study of research topic carried out and has been presented in satisfactory manner to warrant its acceptance as prerequisite to the degree for which it has been submitted.

It is understood that by this approval, the undersigned do not necessarily endorse any conclusion drawn or opinion expressed there in, but approve the thesis for the purpose for which it is submitted.

Dr. Prakash Kumar

Head of Department

Dept. of Production Engineering

B.I.T. Sindri, Dhanbad

(External Examiner)

## **CONTENTS:**

---

<b>Chapter</b>	<b>Title</b>	<b>Page no.</b>
<b>Chapter 1</b>	<b>Introduction</b>	<b>1</b>
1.1	Concept of Wire Arc Additive Manufacturing (WAAM)	1
1.2	Finite Element Modelling (FEM)	2
1.3	Finite Element Analysis (FEA): Governing equation and boundary condition	2
1.4	Various Machine Learning models	3
<b>Chapter 2</b>	<b>Literature Review</b>	<b>8</b>
2.1	Objectives	<b>11</b>
<b>Chapter 3</b>	<b>Research Methodology</b>	<b>12</b>
3.1	Material Properties and Method	12
3.2	Research Methodology Flow diagram	13
3.3	Implementing Machine Learning on the data	14
<b>Chapter 4</b>	<b>Results and Discussion</b>	<b>16</b>
4.1	Training and Testing Results of various ML models	19
4.2	Predicted Surface Temperatures of Known Layers	20
4.3	Forecasted Surface Temperatures of Unknown Layers	21
<b>Chapter 5</b>	<b>Conclusion</b>	<b>23</b>
<b>References</b>		<b>24</b>

## LIST OF FIGURES:

---

Figure No.	Figure Title	Page No.
1.1	Schematic diagram of WAAM.	1
1.2	Structure of a simple decision tree.	4
1.3	Algorithm of a Random Forest model.	5
1.4	Architecture of a LSTM neural network.	5
1.5	Simple 1D CNN architecture with two convolutional layers.	6
1.6	Architecture of Multi-Layer Perceptron model.	6
1.7	Structure of an Automated Machine Learning (AutoML) model.	7
3.1	Meshed model of deposited layers using WAAM	12
3.2	Details of objects in experimental work.	13
3.3	Flow diagram	14
4.1	Surface temperature of 1 <sup>st</sup> , 3 <sup>rd</sup> , 5 <sup>th</sup> , 6 <sup>th</sup> layer	16
4.2	Surface temperature of 4 <sup>th</sup> layer and 6 <sup>th</sup> layer	17
4.3	Heat source and surface temperature distribution in different layers with time	17
4.4	Temperature distribution shown in cut line of vertical axis.	18
4.5	Temperature graph between Experimental work and simulation.	18
4.6	Meshed Temperature distribution with 30 sec idle time in 5th layer	19
4.7	Actual and predicted temperature of layer 6 by Decision Tree Regressor.	20
4.8	Actual and predicted temperature of layer 6 by Random Forest Regressor.	13
4.9	Actual and predicted temperature of layer 6 by AutoML.	14
4.10	Actual and Forecasted temperature of layer 18 by Decision Tree Regressor	14
4.11	Actual and Forecasted temperature of layer 18 by Random Forest Regressor	15
4.12	Actual and Forecasted temperature of layer 18 by AutoML	15

## **LIST OF zaTABLES:**

---

<b>Table No.</b>	<b>Table Title</b>	<b>Page No.</b>
<b>1</b>	Material parameters of Aluminum 6063 T83 alloy	<b>12</b>
<b>2</b>	Mesh statistics of the WAAM model	<b>13</b>
<b>3</b>	Process parameters of various machine learning models.	<b>15</b>
<b>4</b>	Comparative MAE and RMSE of various machine learning models	<b>19</b>

## ABSTRACT

---

Wire and arc additive manufacturing (WAAM) can produce medium to large-size engineering components because of its high rate of deposition. However, while producing the large size components, they can be subject to thermal cycles and the problem of heat accumulation which can result in the reducing the mechanical and microstructural properties of the WAAM components. To understand the behaviour of the heat cycle layer by layer of a large component of aluminium alloys, thermal modelling and simulation are carried out in this work. Layer-by-layer surface temperatures were obtained to understand the temperature field in linear wall fabricated using WAAM.

The simulation result revealed that temperature in the advancing layers increases and surface temperature in the lower layer decrease with time. The moving heat source maximum temperature reached approx. 2400 °C in the 19<sup>th</sup> layer and the surface temperature in the 1<sup>st</sup> layer decreased to 510°C. By Experiment in lab, we easily compare the temperature using thermocouple, either our simulation thermal modelling validates the good result or not. From results we can say, the temperature will increase while making consecutive layers heat are accumulated in the top layers which cause heat management issue. To solve this problem, we gave 30 sec idle time to achieve the room temperature to solve the heat issue management. After the getting the result, we forecast the result through machine learning to predict the temperature of the next top layers of WAAM.

**Keywords:** *WAAM, Thermal Modelling, Finite Element Analysis, Machine Learning (ML).*



## CHAPTER 1: INTRODUCTION

---

### 1.1 Concept of Wire and Arc Additive Manufacturing (WAAM)

Wire and Arc Additive Manufacturing (WAAM) uses a solid wire as feedstock and an electric arc as a heat source to obtain three-dimensional components. WAAM can produce medium to large-size engineering components for various industries such as ship, aerospace, defence, and spacecraft as well construction industry. Due to its high rate of deposition, it has the potential of producing unlimited shape components merely with a minimum cost of setup and execution. The layer-by-layer deposition process of WAAM for creating three-dimensional, intricate, and near-net-shaped parts is a significant driving force for advancements in manufacturing components in recent years. Fabrication of large components using WAAM experiences thermal cycles and heat accumulation, potentially reducing their mechanical and microstructural properties. To study the layer-by-layer heat cycle behaviour of large components fabricated using WAAM, the computational tool can play an important role in solving the problem of thermal cycle and heat accumulation.

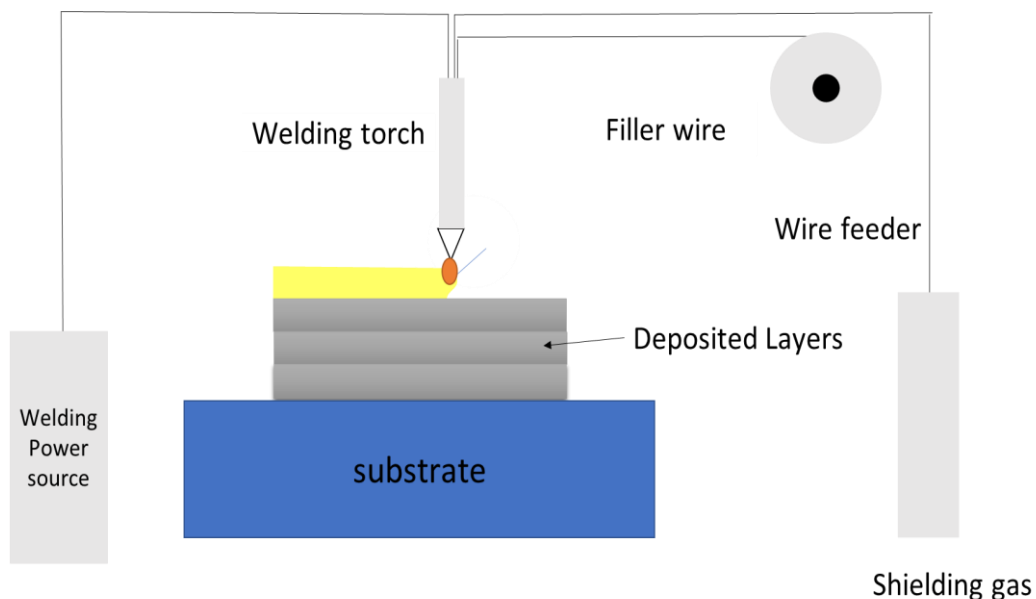


**Fig 1.1** Schematic diagram of WAAM

The effect of substrate preheating using 3D transient heat transfer finite element modelling (FEM) in WAAM was studied. The result of FEM and experiment showed that preheating can help in improving the thermal cycle and decreasing of cooling rate of molten metal. The maximum temperature gradient decreases with increased preheating temperature. FEM is used to obtain an optimal process parameter to improve the deposition efficiency in

WAAM by controlling heat input layer-by-layer in Aluminium alloy. FEA is used for finding the idle time to maintain constant inter-pass temperature and constant melt pool size throughout the deposition process layer-by-layer. A numerical simulation was carried out to obtain optimal bead height and bead width by controlling voltage and hence heat input in the deposited layers.

Additionally, experimental approaches have been applied in large numbers to study the thermal behaviour of WAAM fabricated parts, their characteristics and their effects on mechanical and metallurgical properties. The thermal modelling of WAAM has been explored to a limited extent for Aluminium alloy to date. This paper investigates the thermal behaviour of WAAM fabricated parts layer-by-layer. And hence helps in improving the deposition efficiency and manufacturability of parts using WAAM.

## **1.2 Finite Element Modelling (FEM)**

The finite element method is a numerical technique for solving problems which are described by partial differential equations or can be formulated as functional minimization. A domain of interest is represented as an assembly of finite elements. Approximating functions in finite elements are determined in terms of nodal values of a physical field which is sought. A continuous physical problem is transformed into a discretized finite element problem with unknown nodal values. For a linear problem a system of linear algebraic equations should be solved. Values inside finite elements can be recovered using nodal values.

Two features of the finite element method are worth to be mentioned:

- a. Piece-wise approximation of physical field on finite elements provides good precision even with simple approximating functions (increasing the number of elements we can achieve any precision).
- b. Locality of approximation leads to sparse equation systems for a discretized problem. This helps to solve problems with very large number of nodal unknowns.

## **1.3 Finite element analysis (FEA): Governing equation and boundary condition**

The Fourier equation of the three-dimensional transient non-linear heat transfer equation is given by equation (1).

$$\frac{\partial}{\partial x}(k \frac{\partial T}{\partial x}) + \frac{\partial}{\partial y}(k \frac{\partial T}{\partial y}) + \frac{\partial}{\partial z}(k \frac{\partial T}{\partial z}) + Q = \frac{\partial(\rho C_p T)}{\partial t} \quad \dots\dots (1)$$

Where x, y, and z are coordinates of the cartesian system, k is the thermal conductivity of the material, T is the temperature, Q is the energy generation per unit volume, ρ is density, C<sub>p</sub> is specific heat capacity and t is time.

The heat transfer modelling is based on moving heat sources based on the Gaussian distribution of power density. The Gaussian heat source distribution formula is given:

$$q(t) = \frac{3Q_A}{\pi r_a^2} \exp \left[ - \left( \frac{r(t)}{r_a} \right)^2 \right] \quad \dots\dots (2)$$

$$Q_A = \eta IU - Q_w \quad \dots\dots (3)$$

$$r(t) = x^2 + y^2 + z^2 \quad \dots\dots (4)$$

$$Q = \eta Q_T = \eta IU \quad \dots\dots (5)$$

Where, Q<sub>A</sub>= Heat given by welding heat source, which varies based on the type of welding process used for deposition, Q<sub>w</sub> energy extracted to melt the filler wire, q (t) is the heat flux per unit area, r<sub>a</sub> is the radius of an arc, r (t) is the radius of the heat source received at a defined point in define time. The r (t) is given by eq. (3). Q is the effective heat of the heat source, Q<sub>T</sub> is the total power of the arc, η is the arc efficiency, I is the welding current and U is the welding voltage.

The total amount of heat Q<sub>T</sub> exchange in form of convention and radiation from the welding plate to the surrounding is given by:

$$Q_T = Q_k + Q_r = \beta (T_s - T_o) \quad \dots\dots (6)$$

Where Q<sub>k</sub> is heat due to convection, Q<sub>r</sub> is the heat due to radiation, β is the convection coefficient, T<sub>s</sub> is the instantaneous temperature and T<sub>o</sub> is the surrounding temperature. Further, convection and radiation coefficient can be temperature dependent, which is not considered in this study.

#### 1.4 Various Machine Learning models

ML is an artificial intelligence (AI) technique that allows a machine or system to learn from data automatically and make decisions or predictions without being explicitly programmed. In research, ML is gaining popularity in medical diagnostics, material property prediction, smart

manufacturing, autonomous driving, natural language processing and object. Some ML models are briefly described below.

- a. Decision Tree is one of the most commonly used, practical approaches for supervised learning. It can be used to solve both Regression and Classification tasks with the latter being put more into practical application.

It is a tree-structured classifier with three types of nodes. The Root Node is the initial node which represents the entire sample and may get split further into further nodes. The Interior Nodes represent the features of a data set and the branches represent the decision rules. Finally, the Leaf Nodes represent the outcome. This algorithm is very useful for solving decision-related problems. Due to the continuous character of the target feature we must have a new splitting criterion i.e., variance.

$$Var(x) = \frac{\sum_{i=1}^n (y_i - \bar{y})}{n-1} \quad \dots\dots (7)$$

where  $y_i$  are the single target feature values and  $\bar{y}$  is the mean of these target feature values.

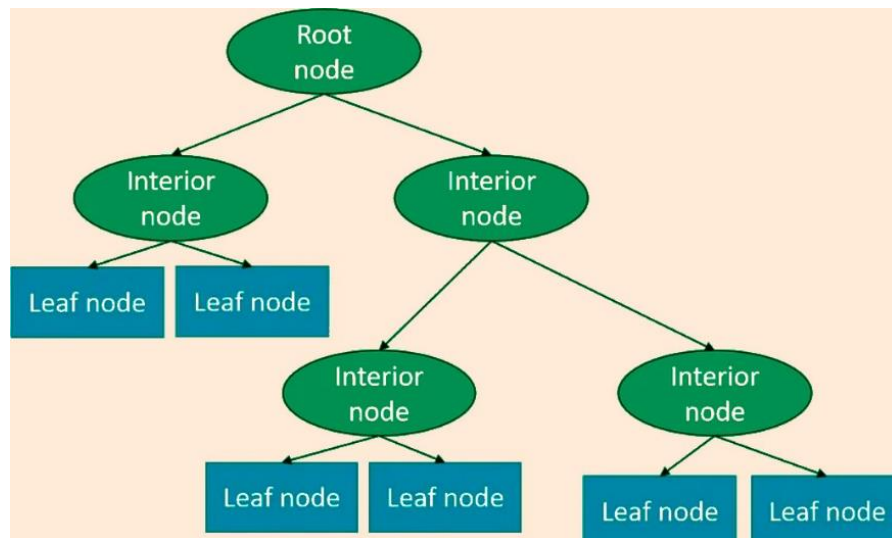


**Fig 1.2** Structure of a simple decision tree.

- b. Random Forest Regression is a supervised learning algorithm that uses ensemble learning method for regression. Ensemble learning method is a technique that combines predictions from multiple machine learning algorithms to make a more accurate prediction than a single model. A Random Forest Regression model is powerful and accurate. It usually performs great on many problems, including features with non-linear relationships. Disadvantages, however, include the following: there is no interpretability, overfitting may easily occur, we must choose the number of trees to include in the model.

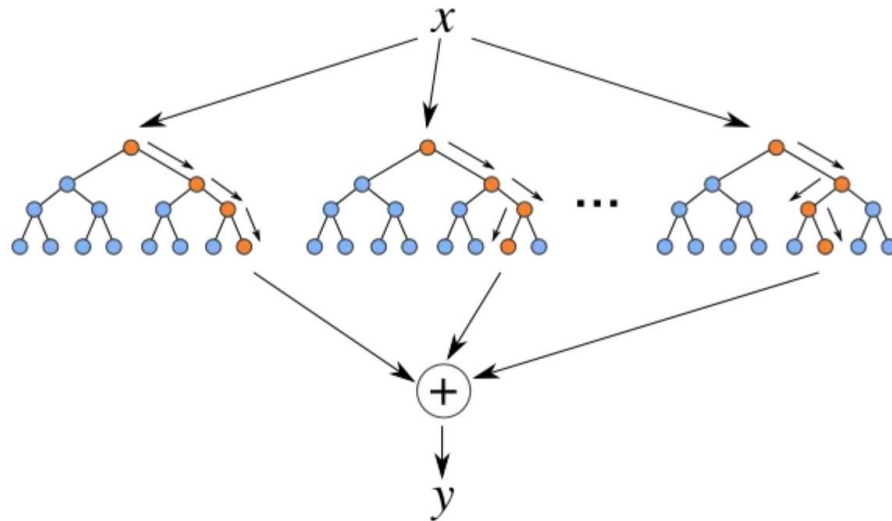


**Fig 1.3** Algorithm of a Random Forest model

- c. To solve the problem of Vanishing and Exploding Gradients in a Deep Recurrent Neural Network, many variations were developed. One of the most famous of them is the Long Short Term Memory network (LSTM). In concept, an LSTM recurrent unit tries to “remember” all the past knowledge that the network is seen so far and to “forget” irrelevant data. This is done by introducing different activation function layers called gates for different purposes. Each LSTM recurrent unit also maintains a vector called the Internal Cell State which conceptually describes the information that was chosen to be retained by the previous LSTM recurrent unit. LSTM algorithm for regression in Machine Learning is typically a time series problem. The critical difference in time series compared to other machine learning problems is that the data samples come in a sequence. The sequence represents a time dimension explicitly or implicitly.

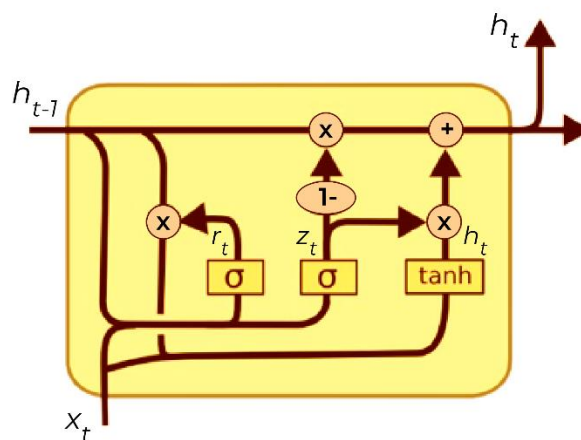


**Fig 1.4** Architecture of a LSTM neural network

$$i_t = \sigma (W_{pi}p_t + W_{hi}h_{t-1} + W_{ci} * c_{t-1} + b_i) \quad \dots\dots (8)$$

$$f_t = \sigma (W_{pf}p_t + W_{hf}h_{t-1} + W_{cf} * c_{t-1} + b_f) \quad \dots\dots (9)$$

$$o_t = \sigma (W_{po}p_t + W_{ho}h_{t-1} + W_{co} * c_t + b_o) \quad \dots\dots (10)$$

- d. CNN is a type of deep learning model for processing data that has a grid pattern, such as images, which is inspired by the organization of animal visual cortex [13, 14] and designed to automatically and adaptively learn spatial hierarchies of features, from low- to high-level patterns.

$$y_{ij}^l = \sigma \left( b_j^l + \sum_{m=1}^M w_{m,j}^l x_{i+m-1,j} \right) \quad \dots\dots (11)$$

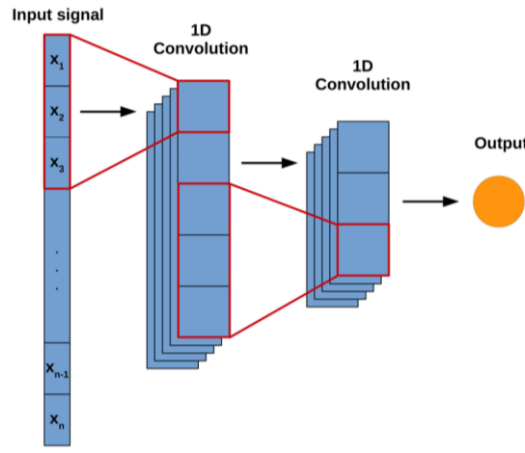


**Fig 1.5** Simple 1D CNN architecture with two convolutional layers.

- e. A multilayer perceptron (MLP) is a feedforward artificial neural network that generates a set of outputs from a set of inputs. An MLP is characterized by several layers of input nodes connected as a directed graph between the input and output layers. MLP uses backpropagation for training the network.

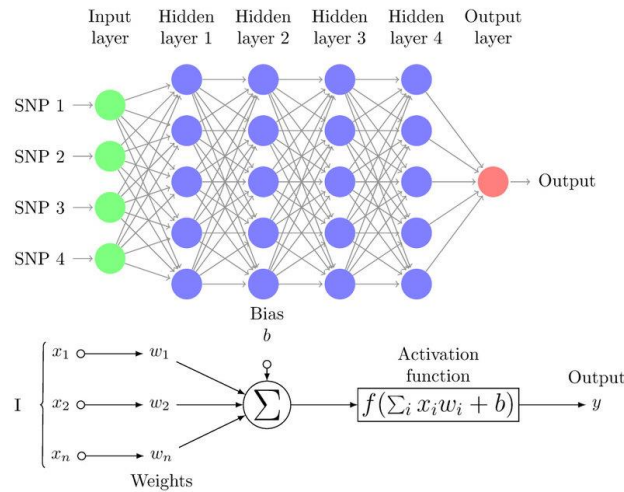


**Fig 1.6** Architecture of Multi-Layer Perceptron model

- f. Automated machine learning (AutoML) is the process of applying various machine learning (ML) models to real-world problems using automation. More specifically, it automates the selection, composition and parameterization of ML models. Automating the machine learning process makes it more user-friendly and often provides faster, more accurate outputs than hand-coded algorithms.

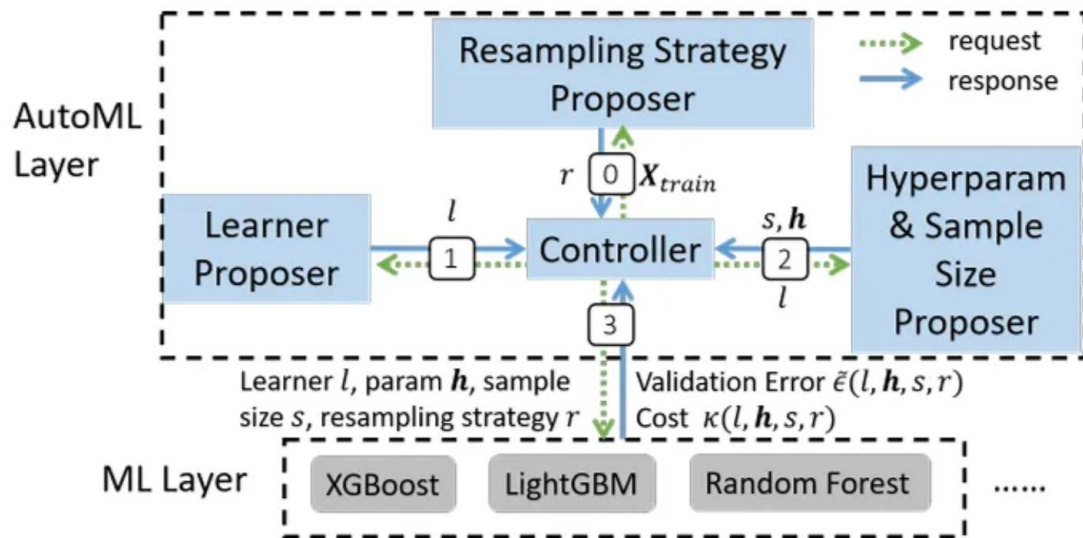


**Fig 1.7** Structure of an Automated Machine Learning (AutoML) model.

## CHAPTER 2: LITERATURE REVIEW

---

Additive manufacturing (AM) technology is based on the principle of discrete-stacking, which has the advantages of directly forming parts with few processing, short production cycle, and high material utilisation, and metal additive manufacturing is an important branch of additive manufacturing technology [1]. With the popularization and widespread application of AM technology, metal additive manufacturing technology is blossoming in the manufacturing industry and has gradually become one of the most promising advanced manufacturing technologies in the field of additive manufacturing. Wire arc additive manufacturing (WAAM) technology is a metal additive manufacturing technology that uses arc as a heat source to process metal solid structural parts by adding materials surface by surface. It has advantages of high deposition efficiency, high wire utilization, and low cost, and can produce large-sized parts. Thus, it has been widely used in aerospace, defence military and energy power industries

**Qian Tang, et al.** [1] Research and application of machine learning for additive manufacturing. To investigate the research and application of ML for AM, a systematic literature review and text mining analysis are adopted for identifying, assessing, and analyzing the literature published between 2000 and 2020. The overall methodology is illustrated in. In the first place, a systematic literature review is adopted to search, select, and assess relevant publications. The systematic literature review is defined as a systematic, explicit and reproducible method for identifying, evaluating, and synthesizing the existing body of completed and recorded work produced by researchers. The review process typically involves several main steps, including specifying research questions, identification of research, selecting and assessing the collected publications.

**Karmuhilan Ma, et al.** [2] In his paper used intelligent process model for bead geometry prediction in WAAM. In this process, generation of layers by depositing beads puts high emphasis on single bead geometry. This paper focuses controlling the bead geometry by suitable selection of welding process parameters. For this artificial neural network (ANN) is modelled to predict the bead parameters based on given process parameters and then the reverse model is designed to select the weld parameters based on user specified bead geometry. The results show that the variable welding parameters are significant, and the ANN model assures the possibility of predicting welding process parameters for desired bead geometry in WAAM application.



**Zhifen Zhanga, et al.** [3] In addition to process modeling, researchers have also explored the use of simulation for optimizing process parameters and reducing defects. For example, Yan et al. (2020) used a genetic algorithm-based optimization method to identify the optimal process parameters for WAAM-deposited Al-12Si, resulting in reduced porosity and improved mechanical properties.

**Won-Jung Oh, et al.** [4] Prediction of deposition bead geometry in wire arc additive manufacturing using machine learning. To reduce the post-processing (machining) in WAAM, this study aimed to address two problems resulting from the deposition direction during GMAW-based WAAM without changing the deposition path or requiring external devices. The first problem is the irregular deposition bead geometry resulting from inappropriate deposition conditions. The second problem is the deviation in the deposition bead geometry between the AS and MD zones. Finally, researchers have also investigated the use of simulation for optimizing the design of WAAM-deposited parts. For example, Qian et al. (2020) used topology optimization and simulation to design a lightweight bracket with improved mechanical performance, demonstrating the potential of using simulation for optimizing the design of complex WAAM-deposited parts.

**Wenqiang Liu, et al.** [5] Compulsively constricted WAAM with arc plasma and droplets ejected from a narrow space. Learn about GMAW and Plasma Arc Welding. Also Morphology of AM layers with different gas flow.

**Xiang He, et al.** [6] Automatic defects detection and classification of low carbon steel WAAM products using improved remanence/magneto-optical imaging and cost-sensitive convolutional neural network. In particular, it is difficult to detect the small defects on the surface and subsurface of the manufactured products. To cope with this issue, we propose a new method for automatic defects detection and classification of low carbon steel WAAM products using improved remanence/magneto-optical imaging and cost-sensitive convolutional neural network. The improved remanence/magneto-optical imaging is used to obtain clear magneto optical images. A convolutional neural network model is then deployed to detect the defects in magneto optical images. The proposed method is effective in automatic detection of the surface defects of low-carbon steel WAAM products.

**Shailendra Pawanr1, et al.** [7] Another important area of research in WAAM simulation is the prediction of the final mechanical properties of the deposited material. Several studies have

developed models for predicting the microstructure and mechanical properties of WAAM-deposited materials based on process parameters and thermal history. For example, Lin et al. (2020) developed a model for predicting the microstructure and mechanical properties of WAAM-deposited Ti-6Al-4V, demonstrating good agreement between the simulation results and experimental measurements.

**Trong-Nhan Le, et al.** [8] One of the most significant challenges in WAAM simulation is accurately modeling the complex multi-physics phenomena that occur during the deposition process. Several studies have focused on developing and validating computational models for simulating the WAAM process. For example, Hu et al. (2021) developed a finite element model for predicting the temperature field, residual stress, and distortion in WAAM-deposited Ti-6Al-4V, demonstrating good agreement between the simulation results and experimental measurements.

## 2.1 Objectives

- a. Finite element analysis
  - i. Development of layer-by-layer thermal modelling of WAAM for large-size aluminum alloy wall using COMSOL Multiphysics.
  - ii. Investigates the thermal behavior of WAAM fabricated parts layer-by-layer.
  - iii. Study of temperature history layer-by-layer
  - iv. Find out the different temperature at fixed point layer by layer.
  - v. Find out the time required to cool down in deposition of layers.
- b. Experimental:
  - i. Compare the simulation result with experimental result
- c. Machine learning
  - i. Develop a Machine Learning (ML) algorithm pipeline for the data driven thermal modelling using data obtained from the simulation.
  - ii. Prediction of layers temperature using developed ML algorithm
  - iii. Compare different algorithm performance

## CHAPTER 3: RESEARCH METHODOLOGY

### 3.1 Materials Properties and Methods

The substrate and filler material was Aluminum 6063 T83 alloy. The material properties of Al 6063 alloy are shown in table 1. As shown in figure 1, the six deposited layers meshed model, designed in commercial Comsol software for FEA. The mesh statistics of the developed WAAM are shown in table 2.

The dimension of the substrate was 70 x 35 x 3 mm<sup>3</sup>. The dimension of the deposited bead was assumed as a rectangular cross-section with dimensions 1 x 3 mm<sup>2</sup> and a length was 60 mm. Each layer takes 20 seconds to complete the deposition. So, the total time taken to complete the deposition of 6 layers was 120 seconds. The idle time taken between the two layers was zero. Assuming the next layer starts immediately after the completion of the last layer takes the same time of 20 seconds to complete the next deposition. Moving heat source temperatures were recorded were obtained at each layer at varying times. The surface temperature (ST) of each layer was recorded when a moving heat source passes the adjacent layer. ST between layers can help in the management of the inter-layer temperature (IT) during layer-by-layer deposition in WAAM.

**Table 1.** Material parameters of Aluminum 6063 T83 alloy

Description (Unit)	Value
Heat capacity at constant pressure (J/(kg·K))	900
Density (kg/m <sup>3</sup> )	2700
Thermal conductivity (W/(m·K))	201
Young's modulus (GPa)	69
Poisson's ratio	0.33

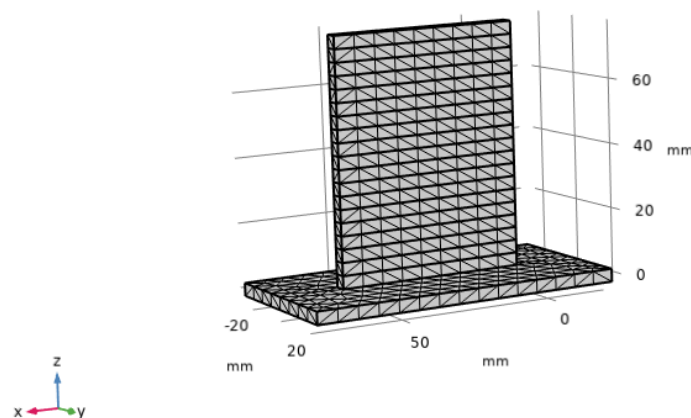


**Fig 3.1** Meshed model of deposited layers using WAAM

**Table 2.** Mesh statistics of the WAAM model

Description	Value
Mesh vertices	1757
Tetrahedra	6428
Triangles	3510
Edge elements	680
Vertex elements	39
Number of elements	6428
Minimum element quality	0.1776
Average element quality	0.5353
Element volume ratio	0.0018411
Mesh volume	16080 mm <sup>3</sup>

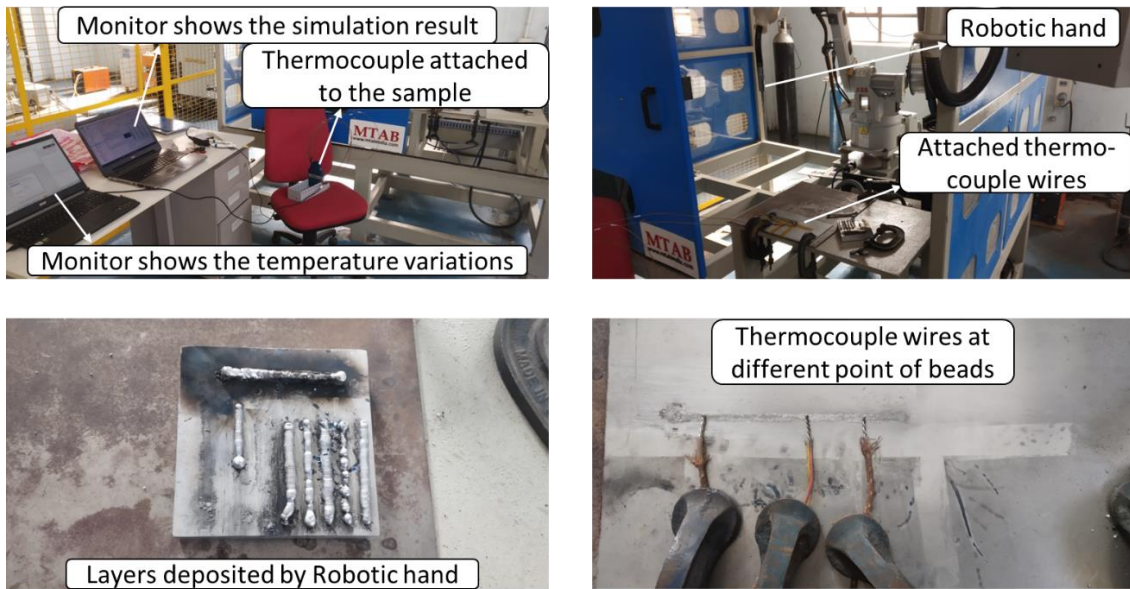


**Fig 3.2** Details of objects in experimental work.

### 3.2 Research Methodology Flow diagram

In this paper, we focused on thermal modeling in Wire Arc Additive Manufacturing through the process of the FEM technique in which the 19 layers are simulated and show the point temperature graph of the mid-point of the layers. A single layer was fabricated on 70 x 35 x 3 mm<sup>3</sup>. The dimension of the deposited bead was assumed as a rectangular cross-section with dimensions 4 x 4 mm<sup>2</sup> and a length was 60 mm. Each layer takes 20 seconds to complete the deposition. So, the total time taken to complete the deposition of 19 layers was 380 seconds. The idle time taken between the two layers was zero. After getting of result through simulation

we validated the result from experimental work in which a robotic hand makes layers in which a thermocouple is attached to the layers to monitor the point temperature between the layers. After which, the result is forecasted through the simulation result and predict temperature of the next layer.

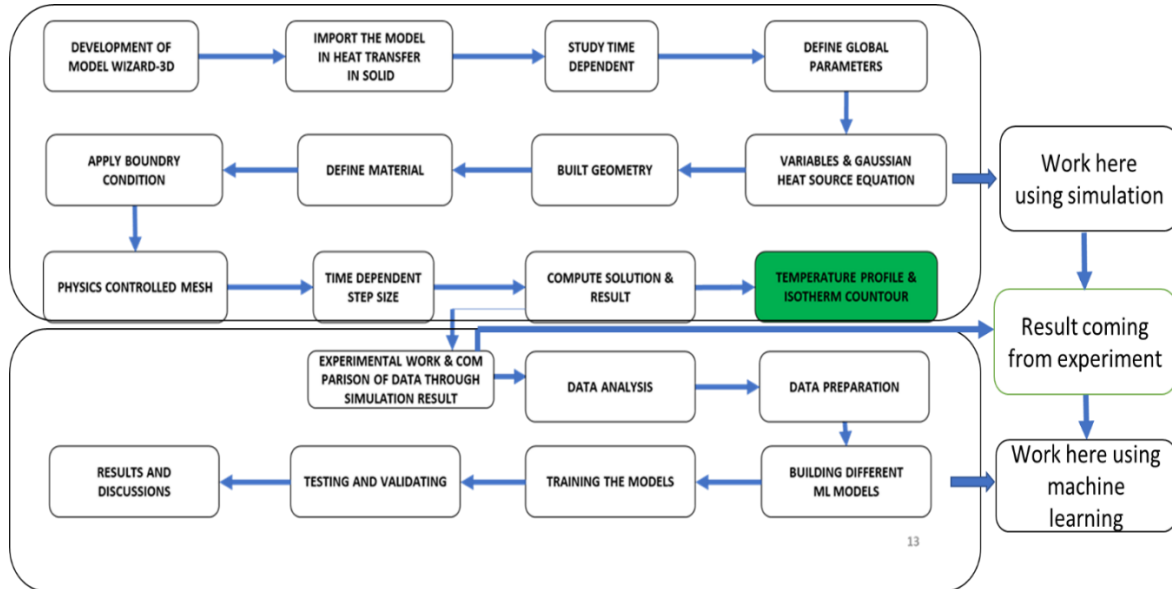


**Fig 3.3** Flow diagram

### 3.3 Implementing Machine Learning on the data

Layer by layer data of temperature distribution with respect to time and different axis was fetched by simulation. This data was complex (shown in the figure below). Therefore, we decided to simplify the data so that we could use it to train and test machine learning models.

We defined and created different machine learning models viz. Decision Tree Regressor, Random Forest Regressor, Multi-Layer Perceptron Regressor, LSTM and tried to fit the training data in each.

The simulation data was simplified so that it become feasible to fit in the various machine learning models. We kept data of layer 1 to 15 for training and testing and kept rest of the data for validating the forecasted surface temperatures. The data of first 15 layers was split into training and testing sets in the ratio of 8:2.

After fitting the training data into all the discussed machine learning models, we further tuned these models with different parameters manually. After tuning the models with appropriate parameters, we compared the Mean Absolute Error (MAE) and Root Mean Square Error (RMSE) of the predicted temperatures of test data from all the models by and analysed the results.

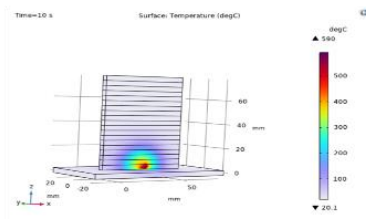
**Table 3.** Process parameters of various machine learning models.

Model	Process Parameters
Decision Tree Regressor	criterion='squared_error', ccp_alpha=10
Random Forest Regressor	ccp_alpha= 0.0, max_depth= 11, max_leaf_nodes= 100, n_estimators= 300, n_jobs= 1, oob_score= False, verbose= 1
MLP Regressor	hidden_layer_sizes=(64, 512, 256, 128),max_iter=4000, beta_1=0.5, beta_2=0.9, tol=0.01, random_state=0, alpha=0.05, validation_fraction=0.1, epsilon=10e-5, learning_rate_init=10e-7
LSTM	loss='mean_absolute_error', optimizer=tf.keras.optimizers.Adam (beta_1=0.9, beta_2=0.1,learning_rate=0.01), epochs=1000, batch_size = 100, workers=3, multiprocessing=True
CNN	loss="mae", optimizer="adam", epochs=1000, batch_size = 25, validation_split=0.1
Auto ML	task="regression",metric='rmse',time_budget=1000, max_iter=3000

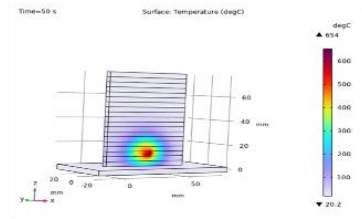
S

## CHAPTER 4: RESULTS AND DISCUSSIONS

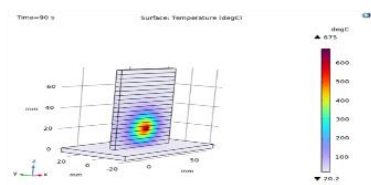
While making consecutive layers, temperature increases and thus heat is accumulated in the adjacent layers. To counter this problem, we found through simulation that 30 sec is the proper idle time to manage the heat issue and thus reduce the temperature in the layers. By the use of a thermocouple, the physical experiment should be validated through temperature variation, and monitoring different points of beads. We used this result for forecasting the temperature variations with respect to time by using various machine learning models of the top layers. The temperature field of the moving heat source increases with the increase of layers with deposition. The deposition time for each layer was taken as 20 seconds. For each layer start time is set as zero, i.e., When no idle time is provided after the start of the next layer. The point temperature (PT) of the heat source at the 1st layer at 10 seconds was 590 °C being the lowest and 2400 °C in the 19th layer being the highest. As shown in figure 2. Heat dissipation is less effective in the upper layers of a deposition process because the heat source is farther from the substrate and can only flow through the previously deposited material. This leads to an accumulation of heat in the deposited structure and an increase in moving heat source temperature. Consequently, increasing the temperature of advancing layers.



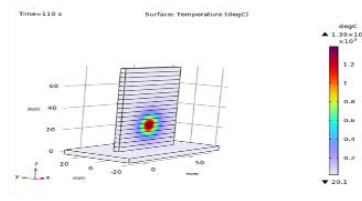
Temperature distribution at 1<sup>st</sup> layer in 10 sec | Max temp.= 590degC



Temperature distribution at 3<sup>rd</sup> layer in 50 sec | Max temp = 654 degC



Temperature distribution at 5<sup>th</sup> layer in 90 sec | Max temp.= 675degC



Temperature distribution at 6<sup>th</sup> layer in 110 sec | Max temp = 1390 degC

**Fig 4.1** Surface temperature of 1<sup>st</sup>, 3<sup>rd</sup>, 5<sup>th</sup>, 6<sup>th</sup> layer (a) 10 sec. (b) 50 sec. (c) 90 sec. and (4) 110 sec.

The ST of the 1<sup>st</sup>, 3<sup>rd</sup>, 5<sup>th</sup>, 6<sup>th</sup> layer at (a) 10sec. (b) 50 sec. (c) 90 sec. and (4) 110 sec are shown in fig 4.1. The maximum value of ST was 2400°C achieved in the 19<sup>th</sup> layer at 380 as



the heat source coincides at the same time. The minimum value of ST was achieved at 590 °C in 10 seconds.

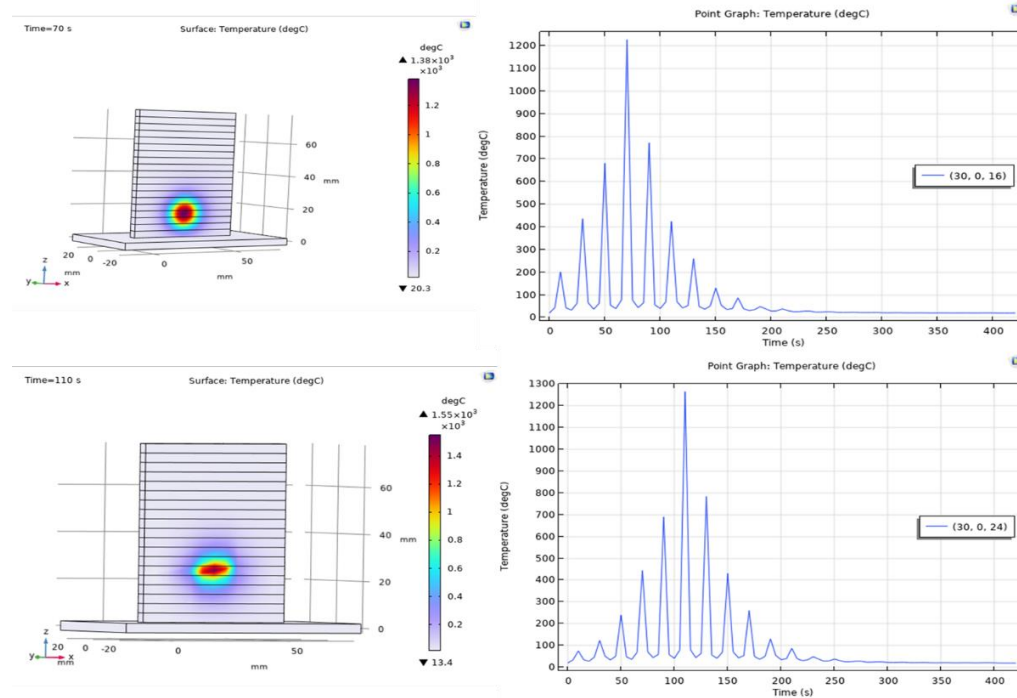


**Fig 4.2** Surface temperature of 4<sup>th</sup> layer and 6<sup>th</sup> layer at (a) 70 sec. (b) 110 sec.

The ST of the 4<sup>th</sup> layer and 6<sup>th</sup> layer at (a) 70 sec. (b) 110 sec. respectively are shown in fig 4.2. The maximum value between the layers of Point Temp. 1390°C was achieved in the 6<sup>th</sup> layer at 110 seconds. Point temperature distribution between the layers also shown in point graph with respect to time.

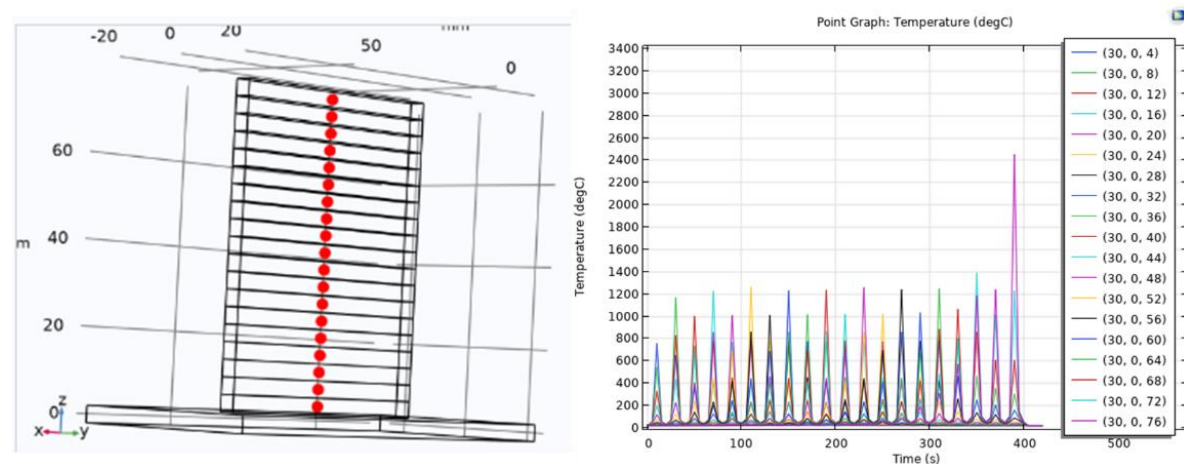


**Fig 4.3** Heat source and surface temperature distribution in different layers with time

In fig 4.3, the graph shows the temperature variation between the layers in the red dot between the layers shows the max. and min. temperature of the layers with respect to time. In

which we can see the max. temperature of the layers is approx. 1210 degC and last layers temperature get rise to the 2400degC due to the coincide the heat source of point temperature with that point.

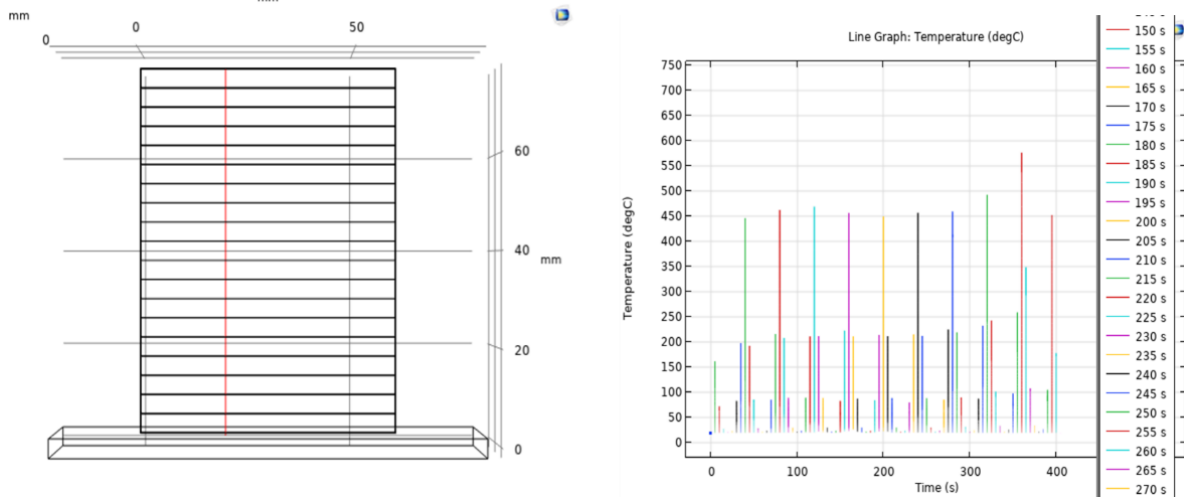


**Fig 4.4** Temperature distribution shown in cut line of vertical axis.

The graph in fig 4.4 shows the vertical temperature along a red line axis between the layers, the graph shows the temperature approx. 560degC max. the min. temperature approx. 310 degC.

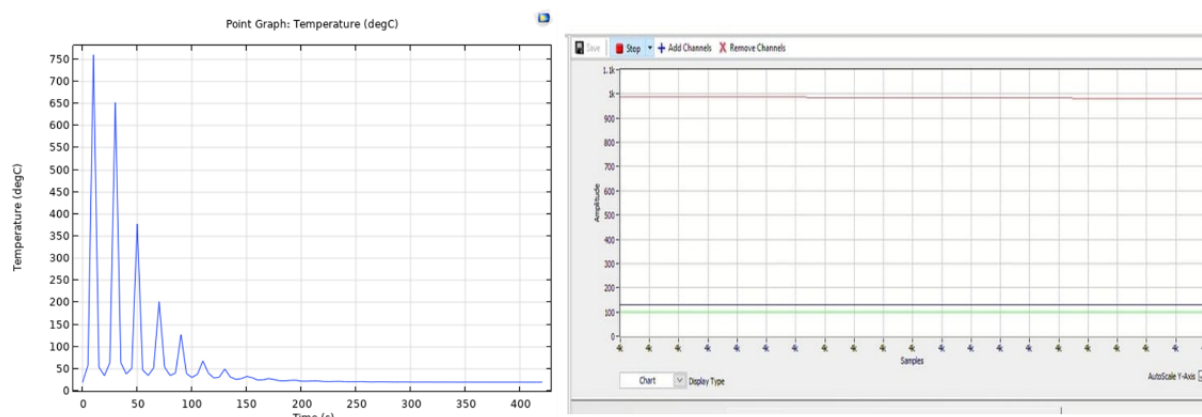


**Fig 4.5** Temperature graph between Experimental work and simulation.

The graph shows the temperature max. 760 degC at first layer of mid-point of layer and this result get by the simulation and the another graph the temperature of the first layer of the bead by the physical experiment through the help of thermocouple is approx. 990 degC.

Fig 4.6 the graph of the 5<sup>th</sup> layer with 30 sec idle time than the max. temperature comes 650 degC and another graph shows the temperature without idle time than the max. temperature comes approx.1000degC.

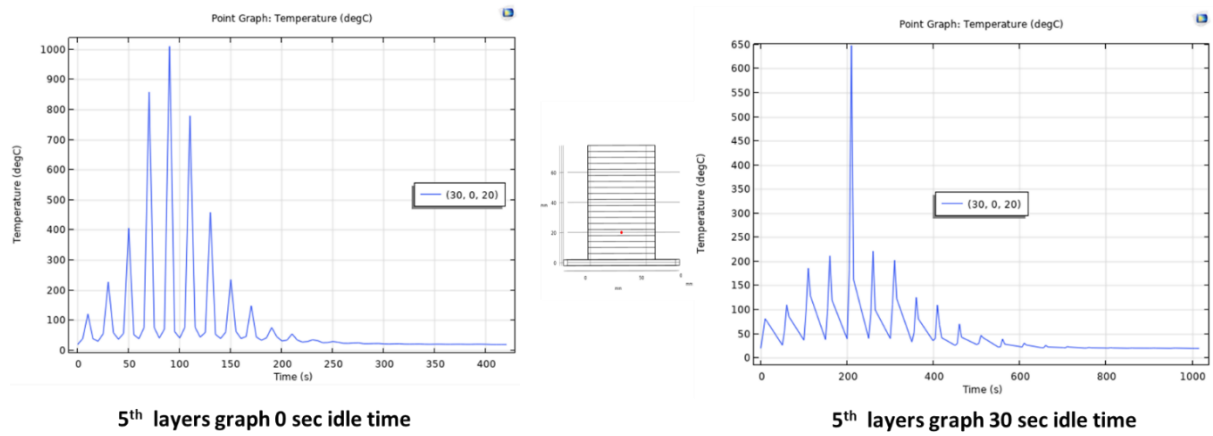


**Fig 4.6** Meshed Temperature distribution with 30 sec idle time in 5th layer

#### 4.1 Training and Testing Results of Machine Learning Models

The performance of the proposed model for forecasting melt pool temperature is evaluated from various metrics. The statistical metrics are utilized to assess the performance of all time-series models. The following commonly used statistical metrics for performance evaluation of time-series models are used.

$$RMSE = \left[ \frac{1}{N} \sum_{i=1}^N (\bar{x}_i - x_i)^2 \right]^{1/2}$$

$$MAE = \frac{1}{N} \sum_{i=1}^N |\bar{x}_i - x_i|$$

**Table 4.** Comparative MAE and RMSE of various machine learning models

Model	MAE	RMSE
Decision Tree Regressor	38.655	130.958
Random Forest Regressor	40.620	111.095
MLP Regressor	72.463	176.951
LSTM	77.276	182.789
CNN	68.712	161.759
Auto ML	22.606	71.035

## 4.2 Predicted Surface Temperature of Known Layers

Fig 4.7, 4.8 and 4.9 shows the training and testing results of predicted temperature in layer 6 by using decision tree regressor, random forest regressor and flaml's automl respectively. These three models among all performed well for fitting and testing the data.

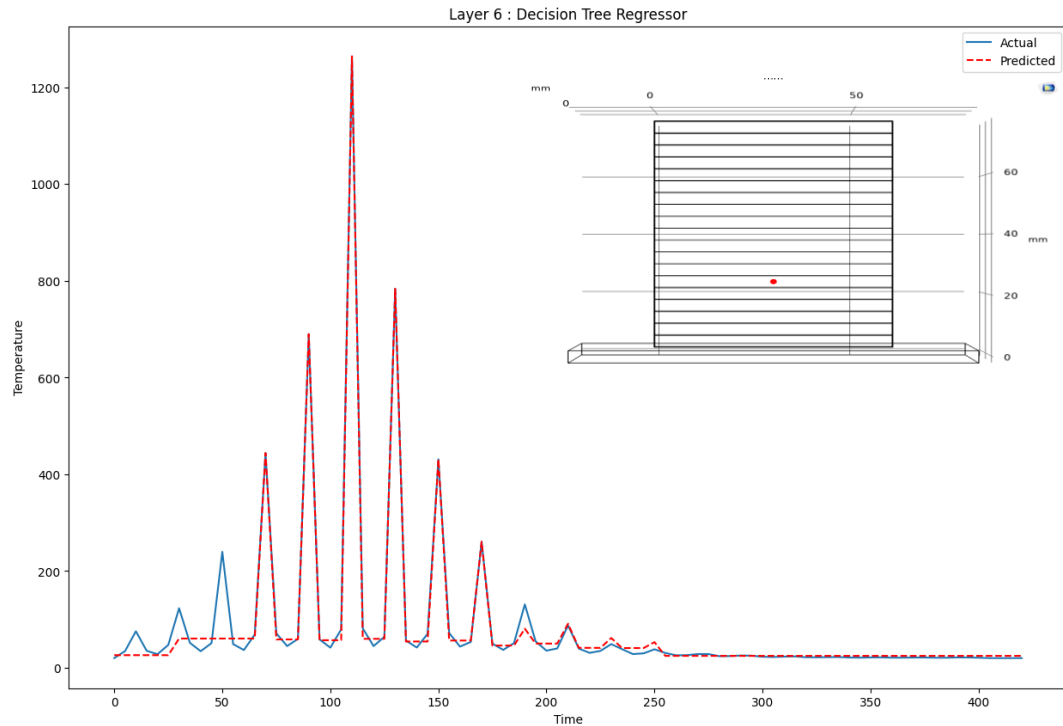


**Fig 4.7** Actual and predicted temperature of layer 6 by Decision Tree Regressor.

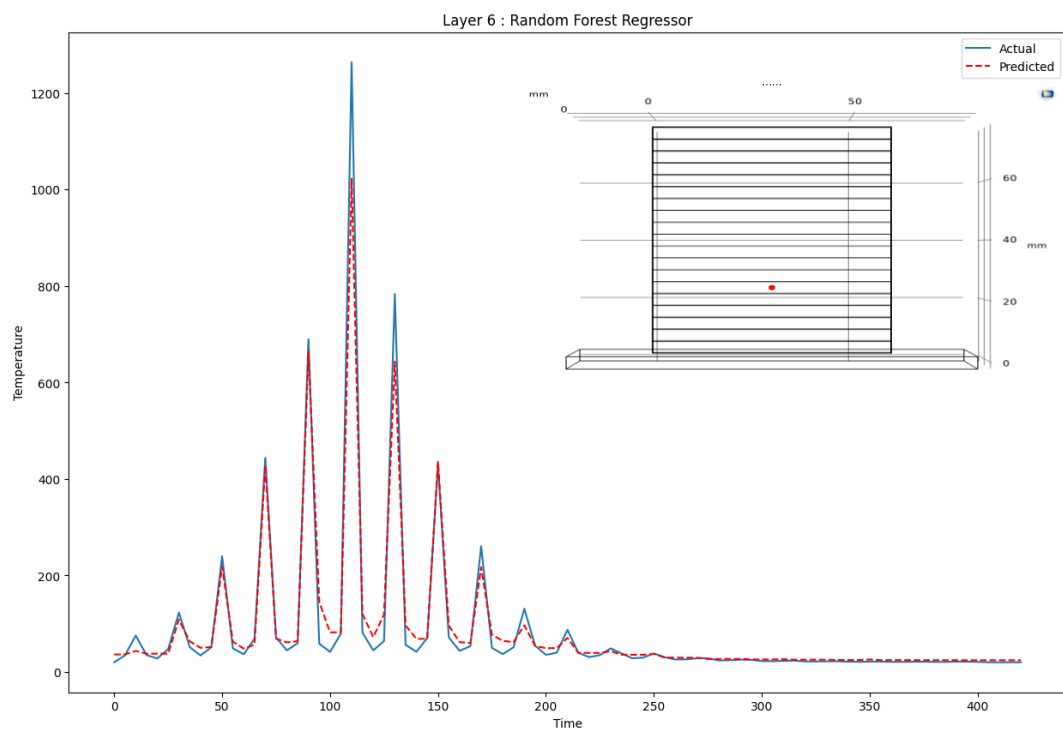


**Fig 4.8** Actual and predicted temperature of layer 6 by Random Forest Regressor.

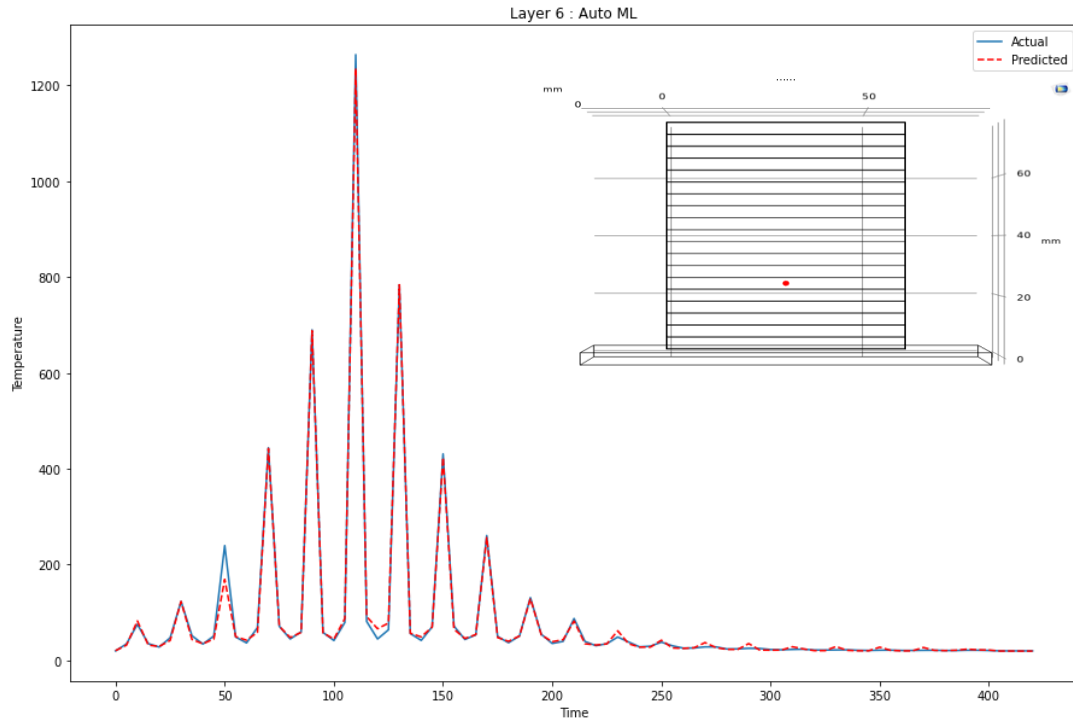


**Fig 4.9** Actual and predicted temperature of layer 6 by Auto ML

### 4.3 Forecasted Surface Temperature of Unknown Layers

Fig 4.10, 4.11 and 4.12 shows the forecasted temperature of layer 18 by using decision tree regressor, random forest regressor and flaml's automl machine learning models respectively. Flaml's automl model among all performed well for forecasting the temperature of unknown layers.

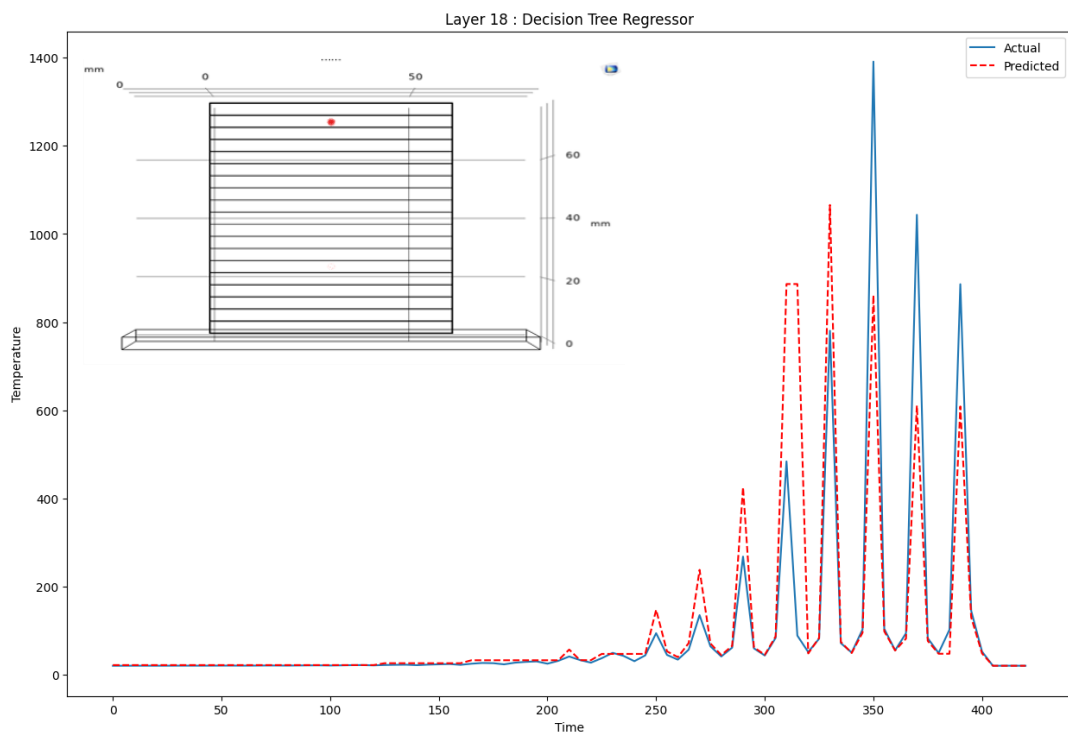


**Fig 4.10** Actual and forecasted temperature of layer 18 by Decision Tree Regressor.

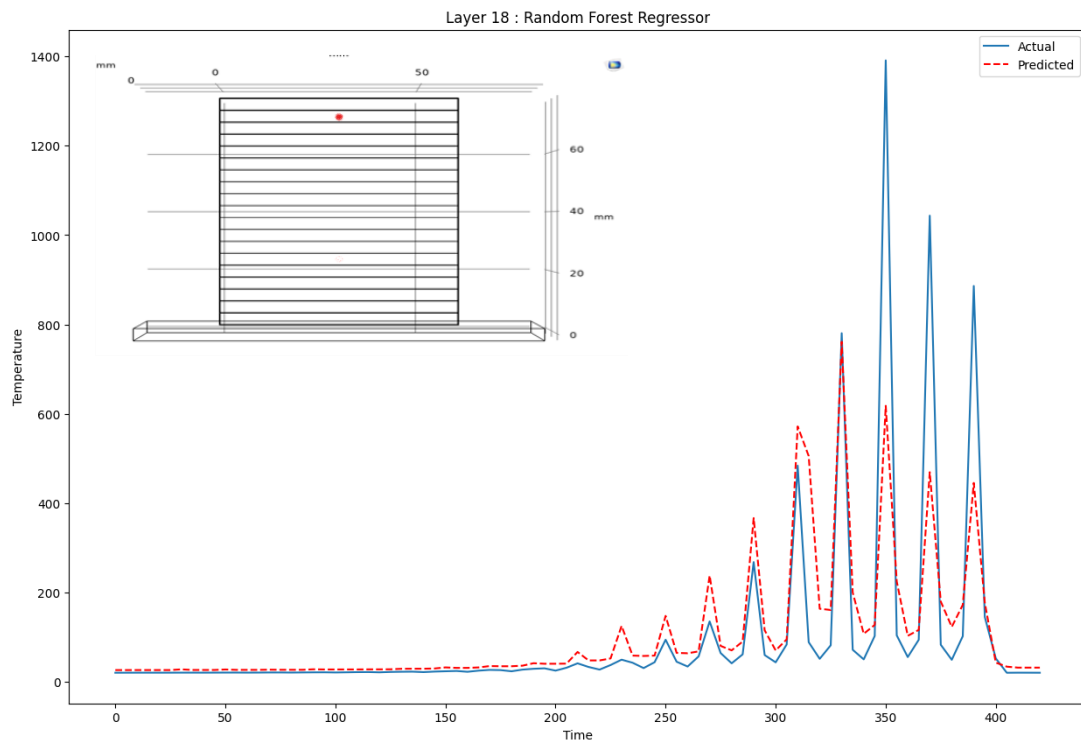


**Fig 4.11** Actual and forecasted temperature of layer 18 by Decision Tree Regressor.

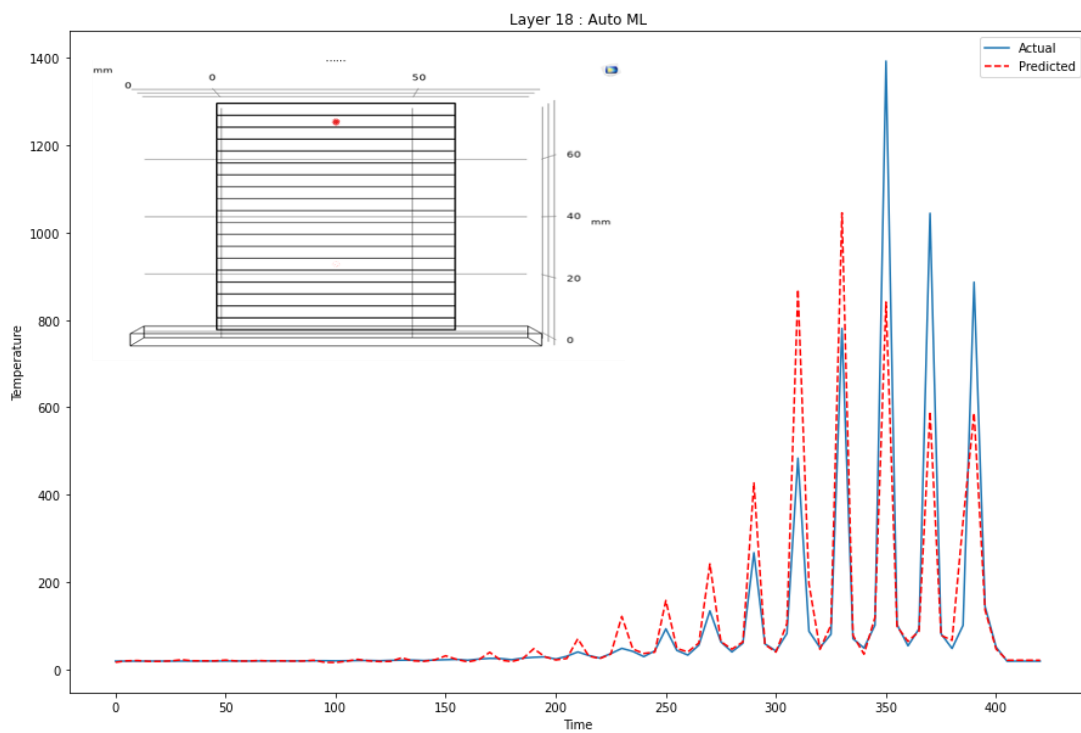


**Fig 4.12** Actual and forecasted temperature of layer 18 by Auto ML.

## CHAPTER 5: CONCLUSION

---

Using finite element software Comsol Multiphysics, a transient heat distribution layer-by-layer in a linear wall fabricated using WAAM was obtained. The FE is the most effective computational tool for the management of heat sources in WAAM fabricated parts. The following conclusion was drawn from the present study of thermal FE in WAAM:

- a. COMSOL multi-physic software is more effective and gives the accurate result of thermal behaviours also it is user friendly software to work on.
- b. During the deposition of layer heat will be accumulated on the plate and it will increase as the height of the layer increases.
- c. We are still working on them to find out the stress produced during the WAAM process and how to optimise this. Also, we should do for the dual time and then find out the result.
- d. In 30 sec idle time all consecutive layers decrease its temperature to the room temperature.
- e. Without idle time the avg. of max. temp of all layers is approx. 1400 degC through the graph.
- f. With 30 sec of given idle the max. temp of all consecutive layers is approx. 650degC through the graph.
- g. By the experimental work the max. temp in layer 1 was approx. 1000 degC and by simulation the max. temperature was approx. 760 degC.
- h. We were able to fit the data into machine learning models with up to r2\_score of 0.98 while training and got r2\_score 0.82 for the testing data.
- i. Decision Trees, Random Forest and AutoML's XGBRegressor models performed pretty well for this kind of data.
- j. We forecasted the temperature of the upper unknown layers using the help of machine learning models and the best r2\_score among these models was 0.56.

## REFERENCES

- [1] A. Gisario, M. Kazarian, F. Martina, and M. Mehrpouya, "Metal additive manufacturing in the commercial aviation industry: A review," *J. Manuf. Syst.*, vol. 53, no. June, pp. 124–149, 2019.
- [2] M. M. Tawfik, M. M. Nemat-Alla, and M. M. Dewidar, "Enhancing the properties of aluminum alloys fabricated using wire + arc additive manufacturing technique - A review," *J. Mater. Res. Technol.*, vol. 13, pp. 754–768, 2021.
- [3] Z. Li *et al.*, "High deposition rate powder- and wire-based laser directed energy deposition of metallic materials: A review," *Int. J. Mach. Tools Manuf.*, vol. 181, no. September, 2022.
- [4] J. Xiong, Y. Lei, and R. Li, "Finite element analysis and experimental validation of thermal behavior for thin-walled parts in GMAW-based additive manufacturing with various substrate preheating temperatures," *Appl. Therm. Eng.*, vol. 126, pp. 43–52, 2017.
- [5] K. Oyama, S. Diplas, M. Mohammed, A. E. Gunnæs, and A. S. Azar, "Heat source management in wire-arc additive manufacturing process for Al- Mg and Al-Si alloys," *Addit. Manuf.*, vol. 26, no. December 2018, pp. 180–192, 2019.
- [6] F. Montevecchi, G. Venturini, N. Grossi, A. Scippa, and G. Campatelli, "Idle time selection for wire-arc additive manufacturing: A finite element-based technique," *Addit. Manuf.*, vol. 21, no. April, pp. 479–486, 2018.
- [7] T. Abe, J. Kaneko, and H. Sasahara, "Thermal sensing and heat input control for thin-walled structure building based on numerical simulation for wire and arc additive manufacturing," *Addit. Manuf.*, vol. 35, no. May, p. 101357, 2020.
- [8] B. Wu, Z. Pan, S. Van Duin, and H. Li, *Thermal Behavior in Wire Arc Additive Manufacturing : Characteristics , Effects and Control*. Springer Singapore, 2019.
- [9] W. Hackenhaar, F. Montevecchi, A. Scippa, and G. Campatelli, "Air-cooling influence on wire arc additive manufactured surfaces," *Key Eng. Mater.*, vol. 813 KEM, pp. 241–247, 2019.
- [10] P. Henckell, M. Gierth, Y. Ali, J. Reimann, and J. P. Bergmann, "Reduction of energy input in wire arc additive manufacturing (WAAM) with gas metal arc welding (GMAW)," *Materials (Basel)*, vol. 13, no. 11, 2020.
- [11] E. Aldalur, A. Suárez, and F. Veiga, "Metal transfer modes for Wire Arc Additive Manufacturing Al-Mg alloys: Influence of heat input in microstructure and porosity," *J. Mater. Process. Technol.*, vol. 297, no. March, p. 117271, 2021.
- [12] J. Goldak, A. Chakravarti, and M. Bibby, "A New Finite Element Model for Welding Heat Sources," vol. 15, no. June, pp. 299–305, 1984.